

Two-photon absorption in CuCl and CuBr under hydrostatic pressure

K. Reimann and St. Rübenacke

Institut für Physik, Universität Dortmund, 44221 Dortmund, Germany

(Received 12 October 1993; revised manuscript received 18 January 1994)

Two-photon absorption is used to measure the shift of the longitudinal Z_3 and $Z_{1,2}$ excitons and the $2P$ exciton in CuCl under hydrostatic pressure. Hydrostatic deformation potentials for excitons and band states are determined with high accuracy. In CuBr the shift of the longitudinal $Z_{1,2}$ exciton is measured, showing a pronounced superlinear pressure dependence. In the high-pressure phase (above 4 GPa) the pressure dependence of luminescence is observed up to 9 GPa in both compounds.

I. INTRODUCTION

Optical experiments in the pressure range above 1 GPa are usually performed with a diamond anvil cell.¹ Because of the small sample sizes required in these cells, most experiments employ linear optical methods (e.g., absorption, reflection, luminescence) for the determination of the pressure dependence of electronic states. We introduce here two-photon absorption (TPA) under hydrostatic pressure for the measurement of excitons in CuCl and CuBr.

In two-photon absorption²⁻⁴ the transition from the initial state to the final state occurs with the simultaneous absorption of two photons. The energy for this transition is thus equal to the sum of both photon energies. In systems with inversion symmetry one- and two-photon transitions are mutually exclusive; one-photon transitions are allowed between states with different parity and two-photon transitions between states with the same parity. In systems without inversion symmetry there may exist transitions which are both one- and two-photon allowed. This is the case for CuCl and CuBr, which crystallize at ambient pressure in the zinc-blende structure (point group T_d). Here all one-photon transitions are also two-photon allowed, but there exist additional two-photon transitions which are forbidden in one-photon absorption. Longitudinal excitons, e.g., are only accessible by two-photon transitions.

The copper halides, especially CuCl, are prototype materials for nonlinear optical experiments.⁵ Recently they have found renewed interest because of the possibility of producing microcrystals.⁶ The electronic band structure of copper halides is characterized by a strong p - d hybridization. The uppermost valence band (Γ_5 symmetry, following the notation of Ref. 7) is composed of atomic Cu d and Cl, Br p states:

$$|\text{VB}\rangle = \alpha|p\rangle + \beta|d\rangle, \quad (1)$$

where α denotes the contribution of p -like and β the contribution of d -like atomic orbitals. The parameters α and β are subject to the normalization condition $\alpha^2 + \beta^2 = 1$. Values for α^2 are given in Table I. The uppermost va-

lence band is predominantly d -like in all copper halides, and the d -like character increases in the sequence CuI, CuBr, CuCl.

Spin-orbit interaction splits the Γ_5 valence band (band gap E_0) into a fourfold (Γ_8 symmetry, orbital momentum $j = \frac{3}{2}$, band gap E_8) and a twofold (Γ_7 symmetry, $j = \frac{1}{2}$, band gap E_7) band. Because of their different degeneracies the band gaps E_8 and E_7 are given by

$$E_8 = E_0 - \frac{1}{3}\Delta_{\text{so}}, \quad (2a)$$

$$E_7 = E_0 + \frac{2}{3}\Delta_{\text{so}}. \quad (2b)$$

The spin-orbit splitting Δ_{so} can be calculated from the atomic spin-orbit splittings Δ_d and Δ_p ,^{8,9}

$$\Delta_{\text{so}} = \alpha^2\Delta_p + \beta^2\Delta_d. \quad (3)$$

In almost all zinc-blende semiconductors, e.g., in CuBr, Δ_{so} is positive, i.e., the Γ_8 valence band has the highest energy. Since Δ_p and Δ_d have opposite sign ($\Delta_p > 0$, $\Delta_d < 0$), we find in the copper halides with their strong d -like contributions a partial compensation of the spin-orbit splitting. In the case of CuCl this even leads to a negative Δ_{so} . Therefore in CuCl the uppermost valence band is twofold with Γ_7 symmetry.

The band states are not directly accessible to experiments. The reasons for this are (i) the Coulomb interaction between electron and hole, which leads to the formation of excitons, and (ii) the interaction of the polarization of these dipole-allowed excitons with the internal electric field, resulting in longitudinal excitons and transverse polaritons.

TABLE I. p -like contribution to the valence band α^2 and spin-orbit splitting Δ_{so} for copper halides at ambient pressure (data taken from Ref. 25).

	α^2	Δ_{so} (meV)
CuCl	0.24	-81
CuBr	0.36	+150
CuI	0.50	+640

The spin-orbit-split Γ_8 and Γ_7 valence bands give rise to two exciton series, the so-called $Z_{1,2}$ and Z_3 excitons.¹⁰ Linear optical experiments can only probe transverse polaritons. These show a very pronounced dependence of energy on wave vector, which makes the analysis difficult. Absorption measurements have also another disadvantage, namely the very high absorption in the exciton resonances. Thus, one has to use either thin films (thickness ~ 100 nm), which lead in high-pressure experiments to very nonhydrostatic pressure conditions,^{9,11} or one can with bulk samples measure only the low-energy tail of the exciton absorption.^{12–15} In contrast to linear optical experiments, TPA allows the selective excitation of longitudinal excitons whose energies are wave vector independent. With TPA it is also possible to excite $2P$ excitons, thus allowing the determination of the pressure dependence of the exciton binding energy. Because of these advantages we use TPA for the study of exciton states in CuCl and CuBr under pressure.

The observation of excitonic spectra in the zinc-blende phase is limited by a pressure-induced phase transition into a tetragonal structure, which occurs both in CuCl and in CuBr at about 4 GPa. In this phase we could measure the pressure dependence of the luminescence up to a pressure of 9 GPa.

II. EXPERIMENT

The classical method^{3,5,16} for the measurement of TPA is to detect a change in the intensity of the transmitted light of the first beam during the presence of the second (high-intensity) beam. This method is, however, not sensitive enough to detect TPA in our thin (about 30 μm thick) samples. In contrast, samples in the aforementioned experiments were several millimeters thick. Therefore in our case TPA is detected by monitoring the free-exciton luminescence from the lower polariton branch¹⁷ as a function of two-photon energy, which is equal to the sum of the two photon energies. Since we use two photons from the same laser, the two-photon energy is equal to twice the laser photon energy.

The experimental setup for these measurements consists of an exciting laser, a cryostat with the sample inside a diamond anvil cell for pressure generation, and the detection system. Since nonresonant (the photon energies are far from resonances, as in our experiments) two-photon absorption in these compounds is a very weak effect, high excitation intensities of about 10 MW/cm² must be used. They are generated by a Nd:YAG-laser-pumped tunable dye laser (where YAG is yttrium aluminum garnet) with a pulse width of 5 ns and a repetition rate of 10 Hz.

The samples were undoped single crystals, cleaved to dimensions of about $100 \times 100 \times 30 \mu\text{m}^3$. For the high-pressure experiments they are placed into a gasketed diamond anvil cell^{1,18} together with ruby powder for pressure determination.^{19,20} To ensure the best possible hydrostatic conditions at low temperatures helium is used as pressure medium. For loading, the cell is immersed into superfluid helium. For our measurements, the cell

is placed in a flow cryostat and cooled down to a temperature T of 6 K. In order to minimize uniaxial stress, which would result in a splitting and/or broadening of the exciton lines, pressure changes are always made at room temperature.²¹

The detection system consists of an $f/1.8$ collection optics, a 1-m-focal-length spectrometer and a GaAs photomultiplier. The wavelength of the spectrometer is held fixed at the (pressure-dependent) free-exciton luminescence, which is determined for every pressure by measuring the luminescence spectrum with above-band-gap excitation. The output signal from the photomultiplier is fed into a gated integrator and sent via an analog-digital converter to a personal computer, which also controls the scanning of the dye laser.

III. RESULTS AND DISCUSSION

A. Zinc-blende phase

1. CuCl

In CuCl we have determined the pressure dependences of the longitudinal Z_3 and $Z_{1,2}$ excitons (the $1S$ excitons) and of the $2P$ exciton of the Z_3 exciton series in the stability range of the zinc-blende phase (0–4 GPa). Figure 1 shows spectra of the Z_3 exciton at different pressures P . One finds a blueshift of the exciton with pressure. Additionally, a broadening of the exciton line is observed. This broadening is probably due to residual uniaxial stress. From measurements by Fröhlich *et al.*²² we can estimate this uniaxial stress to be less than 1% of the hydrostatic pressure. A plot of the energies of the Z_3 exciton versus pressure is given in Fig. 2 together with the energies of $Z_{1,2}$ and $2P$ excitons. For all resonances in CuCl a linear shift to higher energies with pressure is observed; Table II lists the measured energies and pres-

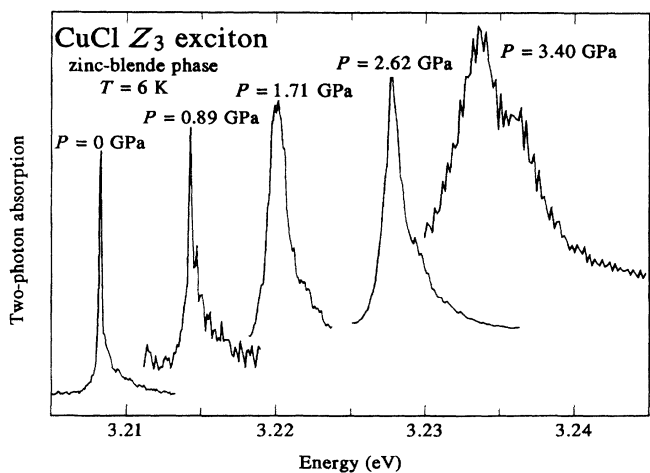


FIG. 1. Two-photon-absorption spectra of the longitudinal Z_3 exciton in CuCl for different pressures at a temperature of 6 K. The energy here and in Figs. 2 and 3 is twice the photon energy of the exciting laser.

TABLE II. Zero-pressure values and linear and quadratic (only for CuBr) pressure coefficients of exciton energies and band parameters in CuCl and CuBr determined by two-photon absorption at a temperature of 6 K.

	$E(P=0)$ (eV)	dE/dP (meV/GPa)	d^2E/dP^2 (meV/GPa ²)
CuCl			
Z_3	3.2076 ± 0.0003	7.65 ± 0.1	0
$Z_{1,2}$	3.289 ± 0.001	6.3 ± 0.5	0
$2P$	3.370 ± 0.001	4.7 ± 0.2	0
R	0.139 ± 0.001	-2.5 ± 0.2	0
E_7	3.405 ± 0.001	4.1 ± 0.2	0
E_8	3.486 ± 0.002	2.8 ± 0.6	0
E_0	3.459 ± 0.002	3.2 ± 0.4	0
Δ_{so}	-0.081 ± 0.002	1.3 ± 0.5	0
CuBr			
$Z_{1,2}$	2.9774 ± 0.0002	3.74 ± 0.04	0.53 ± 0.04

sure coefficients.

The $Z_{1,2}$ exciton has a smaller pressure coefficient than the Z_3 exciton. With the assumption²³ of equal exciton binding energies the spin-orbit splitting (see Table II) is just the energy difference between $Z_{1,2}$ and Z_3 excitons:

$$\Delta_{so} = E_{Z_3} - E_{Z_{1,2}}. \quad (4)$$

Thus, the absolute value of the (negative) spin-orbit splitting decreases with pressure.

Since the pressure coefficient for the $2P$ exciton is

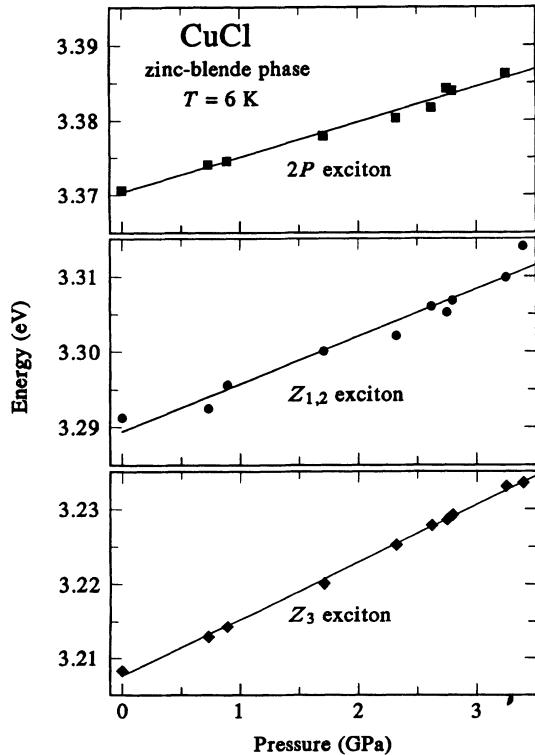


FIG. 2. Energies of longitudinal Z_3 and $Z_{1,2}$ excitons and of the $2P$ exciton in CuCl as function of pressure.

smaller than the pressure coefficient for the Z_3 exciton, the exciton binding energy also decreases with pressure. For a quantitative analysis of the pressure dependence of the exciton binding energy one has to take into account the fact that the exciton series is not hydrogenlike because of strong screening effects.²⁴ In CuCl the Z_3 ($1S$) exciton energy is not

$$E_{Z_3} = E_7 - R, \quad (5)$$

but instead

$$E_{Z_3} = E_7 - 1.42R, \quad (6)$$

where R is the exciton Rydberg energy, which is determined from the energies of $2S$ and $3S$ excitons.²⁵ Equation (6) allows one to calculate the exciton Rydberg energy R and the band gaps E_7 , E_8 , and E_0 from the measured exciton energies:

$$R = \frac{1}{1.42 - 0.25} (E_{2P} - E_{Z_3}), \quad (7a)$$

$$E_7 = E_{Z_3} + 1.42R, \quad (7b)$$

$$E_8 = E_{Z_{1,2}} + 1.42R, \quad (7c)$$

$$E_0 = \frac{1}{3}E_7 + \frac{2}{3}E_8. \quad (7d)$$

The results are given in Table II.

For a comparison with theoretical investigations it is convenient to transform from a pressure to a volume (V) dependence,^{26,27} which gives the hydrostatic deformation potentials a . In first order the pressure-volume relationship is given by the bulk modulus B :

$$B = -V \frac{dP}{dV}. \quad (8)$$

This leads to the following expression for the exciton deformation potential a_{Z_3} :

$$a_{Z_3} = V \frac{dE_{Z_3}}{dV} = -B \frac{dE_{Z_3}}{dP}. \quad (9)$$

The expressions for the deformation potentials $a_{Z_{1,2}}$ and a_{2P} are analogous. Values calculated with a bulk modulus^{28,29} of $B = 45.9$ GPa are given in Table III.

More important than the exciton deformation potentials given above are the deformation potentials a_1 and a_2 , which describe the volume dependence of the band structure. They are defined by³⁰

$$a_1 = V \frac{dE_0}{dV}, \quad (10a)$$

$$a_2 = -\frac{V}{3} \frac{d\Delta_{so}}{dV}. \quad (10b)$$

Table III shows our results for a_1 and a_2 together with the results of other authors. Compared to the measurements of Blacha *et al.*¹¹ and Anthony *et al.*³¹ we find a much smaller deformation potential a_1 , in spite of similar values for the exciton deformation potentials. The reason for this is that these authors neglected the pressure dependence of the exciton binding energy. Our measurements show, however, that the pressure dependences of the band gap and of the exciton binding energy are of

TABLE III. Deformation potentials (in eV) for CuCl and CuBr in the zinc-blende phase.

		Reference
CuCl		
a_{Z_3}	-0.351 ± 0.005	This work ^a
	-0.445 ± 0.05	11 ^b
	-0.4	31 ^c
	-1.00 ± 0.09	13 ^d
	-0.31 ± 0.02	11 ^e
$a_{Z_{1,2}}$	-0.29 ± 0.02	This work ^a
	-0.355 ± 0.05	11 ^b
	-0.4	31 ^c
a_{2P}	-0.22 ± 0.01	This work ^a
a_1	-0.15 ± 0.02	This work ^a
	-0.39 ± 0.04	11 ^b
	-0.4	31 ^c
a_2	0.021 ± 0.008	This work ^a
	0.03 ± 0.02	11 ^b
	0.037 ± 0.01	9 ^f
CuBr		
$a_{Z_{1,2}}$	-0.170 ± 0.002	This work ^a
	-0.30 ± 0.05	11 ^b
	-0.2 ± 0.2	31 ^c
	-0.39 ± 0.04	14 ^d
	-0.18 ± 0.03	11 ^e
	-0.26 ± 0.08	36 ^g

^aTwo-photon absorption, $T = 6$ K.

^bAbsorption, thin films, $T = 100$ K.

^cAbsorption, thin films, $T = 90$ K.

^dAbsorption, bulk samples, $T = 300$ K.

^eLuminescence, $T = 100$ K.

^fAbsorption, thin films, $T = 200$ K.

^gReflection under uniaxial stress, $T = 1.8$ K.

similar size.

Because of the strong p - d hybridization the deformation potentials of CuCl are very small compared to other I-VII compounds. As an example, the hydrostatic deformation potential³² a_1 of KI, which has a pure p -like valence band, is $a_1 = -2.2$ eV, compared to $a_1 = -0.15$ eV in CuCl.

From the pressure-induced change of spin-orbit splitting we are able to estimate the change of p - d hybridization with pressure by using Eq. (3). We take from literature^{8,25} the parameters

$$\begin{aligned} \alpha^2 &= 0.24 \quad (\text{at zero pressure}), \\ \Delta_p &= 0.095 \text{ eV}, \\ \Delta_d &= -0.137 \text{ eV}. \end{aligned} \quad (11)$$

The derivative of Eq. (3) with respect to pressure yields with $\alpha^2 + \beta^2 = 1$:

$$\frac{d\Delta_{so}}{dP} = \frac{d\alpha^2}{dP} (\Delta_p - \Delta_d). \quad (12)$$

Hence it follows that

$$\frac{d\alpha^2}{dP} = (6 \pm 2) \times 10^{-3} \text{ GPa}^{-1}. \quad (13)$$

Thus, the p -like contribution increases from $\alpha^2 = 0.24$ at zero pressure to $\alpha^2 = 0.264$ at 4 GPa. Although this change in p - d mixing is quite small, it is nevertheless important, because it partly compensates the pressure-induced increase of Cu- s -halogen- p interaction, thus leading to a small deformation potential a_1 . This result is supported by tight-binding band structure calculations,²⁷ which take into account the p - d admixture in a straightforward way.

2. CuBr

In CuBr we have measured the $Z_{1,2}$ exciton in the zinc-blende phase from 0 to 4 GPa. The observation of the Z_3 exciton was not possible because this resonance is degenerate with continuum states of the $Z_{1,2}$ exciton series. Therefore it is not possible for us to determine in CuBr the pressure dependences of the spin-orbit splitting and of the p - d hybridization.

In contrast to the case of CuCl, the $Z_{1,2}$ exciton in CuBr shows a superlinear shift with pressure (see Fig. 3). The results of a quadratic fit are listed in Table II, and the exciton deformation potential $a_{Z_{1,2}}$ is given in Table III. For the calculation of $a_{Z_{1,2}}$ we have used a bulk modulus^{33,34} $B = 45.5$ GPa. The quadratic pressure dependence may be due to k -linear terms,^{35,36} which would result in a mixing of $Z_{1,2}$ and Z_3 excitons. Since this

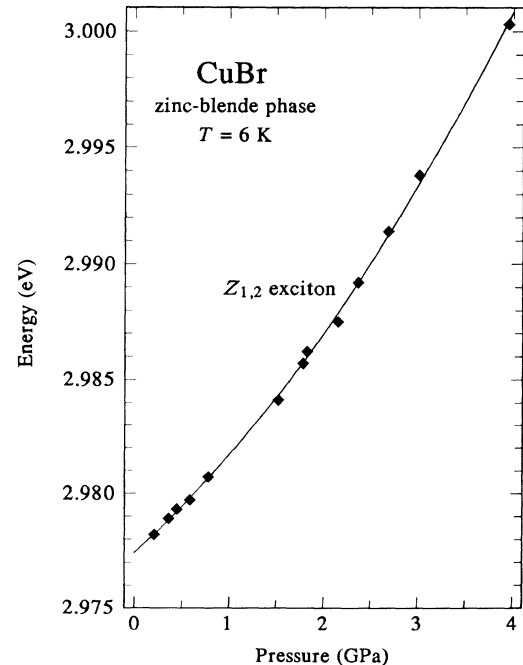


FIG. 3. Energy of the longitudinal $Z_{1,2}$ exciton in CuBr as function of pressure.

mixing is due to off-diagonal terms in the Hamiltonian, a linear change with pressure of matrix elements leads to a quadratic pressure shift for the energies.

B. Tetragonal phase

Both CuCl and CuBr exhibit at about 4 GPa a structural phase transition from the cubic zinc-blende structure to a tetragonal structure, probably the PbO structure.^{11–14} At even higher pressures another phase transition to the rocksalt structure^{11–13} takes place. We did not observe this rocksalt phase for pressures up to 9 GPa in contrast to Ves *et al.*,¹⁴ who observed the rocksalt phase for CuBr already at a pressure of 7.7 GPa. The reason for this difference in transition pressure is probably the large amount of uniaxial stress in the experiment of Ves *et al.*¹⁴ (they did not use any pressure medium), which tends to decrease transition pressures.

We have measured luminescence spectra for both substances in the tetragonal phase in the pressure range 4–9 GPa. For CuCl we have used two-photon excitation by the second harmonic (wavelength 532 nm, photon energy 2.32 eV), for CuBr one-photon excitation by the third harmonic of a Nd:YAG laser (wavelength 355 nm, photon energy 3.49 eV). To find out whether the type of excitation (one- or two-photon excitation) makes any difference in the luminescence spectra, we have in CuCl measured also some spectra with one-photon excitation. We find that the spectra are independent of the type of excitation.

Figure 4 shows two luminescence spectra for CuCl in the tetragonal phase at different pressures. We assign the peak at the high-energy side of the luminescence spectrum to the band gap. The tail at the low-energy side is due to defects, which are generated by the structural phase transition. For CuCl the band gap shifts linearly with pressure as shown in Fig. 5. The pressure coefficient is listed in Table IV and compared with earlier ab-

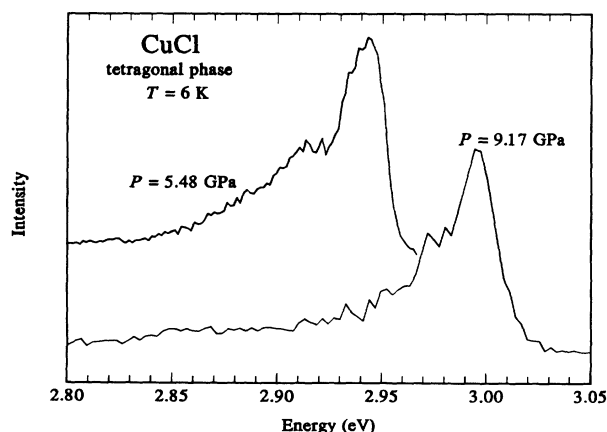


FIG. 4. Luminescence spectra of tetragonal CuCl for different pressures at a temperature of 6 K, using two-photon excitation with a photon energy of 2.32 eV. The energy here and in Figs. 5 and 6 is the photon energy of the emitted photon.

TABLE IV. Pressure dependence of the band gap in the tetragonal phases of CuCl and CuBr.

$E(6 \text{ GPa})$ (eV)	dE/dP (meV/GPa)	
CuCl		
2.948 ± 0.003^a	14.7 ± 0.3^a	
2.97^b	14^b	
2.9^c	21.0^c	
CuBr		
2.5242 ± 0.0008^a	0^a	$P < 6.3 \text{ GPa}$
	6.4 ± 0.2^a	$P > 6.3 \text{ GPa}$
2.95^b	-17^b	
2.49^d	7.4^d	

^aThis work, luminescence, $T = 6 \text{ K}$.

^bRef. 11, absorption, thin films, $T = 100 \text{ K}$.

^cRef. 13, absorption, bulk samples, $T = 300 \text{ K}$.

^dRef. 14, absorption, bulk samples, $T = 300 \text{ K}$.

sorption experiments. The pressure coefficient for CuCl is in good agreement with absorption measurements on thin films.¹¹ The zero-pressure energy of the luminescence is Stokes-shifted by about 50 meV compared to the lowest absorption peak. Hence it is a reasonable assumption to assign the observed luminescence to a direct band gap. Absorption measurements on bulk samples at room temperature,¹³ which measure the low-energy tail (Urbach tail) of the band gap, yield a larger pressure coefficient (21.0 vs 14.7 meV/GPa) than our measurements.

In contrast to CuCl the luminescence peak of the high-pressure phase of CuBr (see Fig. 6) does not show a simple linear pressure dependence. Up to a pressure of

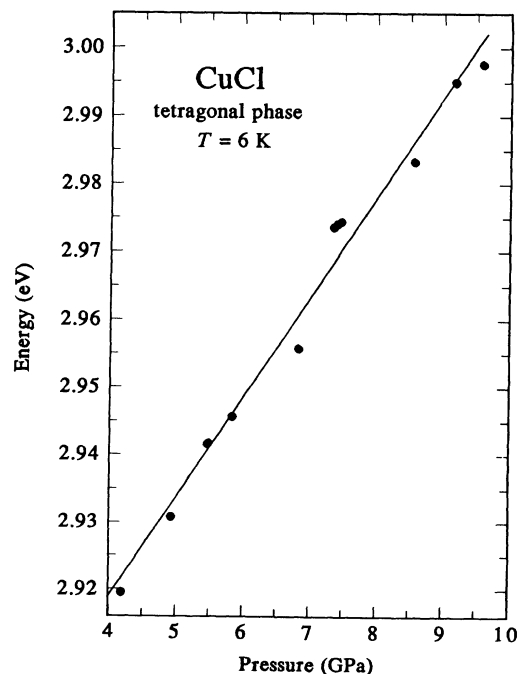


FIG. 5. Band gap (luminescence peak) of tetragonal CuCl as function of pressure.

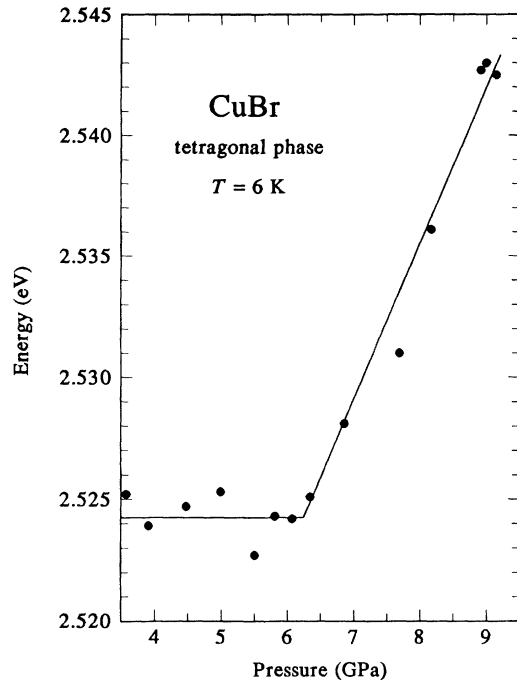


FIG. 6. Band gap (luminescence peak) of tetragonal CuBr as function of pressure.

6.3 GPa the energy stays constant at (2.5242 ± 0.0008) eV. At higher pressures the luminescence line shifts linearly; the pressure coefficient is listed in Table IV. This behavior may be connected with pressure-induced changes in the crystal structure. Either a second phase transition may occur at 6.3 GPa or up to this pressure the internal structural parameter (i.e., the positions of the atoms in the unit cell) changes and so compensates the band-gap increase due to the pressure-induced decrease in crystal

volume.

If one compares our results for the band gap in the tetragonal phase of CuBr above 6.3 GPa with results of other authors, we find reasonable agreement with absorption measurements on bulk samples,¹⁴ but not with absorption measurements on thin films.¹¹ In thin films the absorption line has a higher energy than the luminescence we observed (2.95 vs 2.5242 eV) and also the pressure coefficient is completely different (even in sign). A possible explanation for this difference is that CuBr in this phase has an indirect gap at 2.52 eV and a direct gap at 2.95 eV. Both bulk absorption and luminescence would then detect the indirect gap while thin-film absorption only shows the direct gap.

IV. CONCLUSION

We have used two-photon-absorption spectroscopy under pressure to determine accurately exciton energies in zinc-blende CuCl and CuBr. Using these data we can calculate hydrostatic deformation potentials and the change of p - d admixture in the valence band of CuCl. In CuCl, we have also determined the pressure dependence of the exciton binding energy. By comparison of our luminescence data with absorption measurements we propose a direct gap for the tetragonal phase of CuCl and an indirect gap for the tetragonal phase of CuBr.

ACKNOWLEDGMENTS

We are grateful to Professor Dr. D. Fröhlich for his steady interest and helpful advice and to Dr. K. Syassen (Max-Planck-Institut für Festkörperforschung, Stuttgart) for the generous loan of the high-pressure apparatus.

¹ A. Jayaraman, *Rev. Mod. Phys.* **55**, 65 (1983); *Rev. Sci. Instrum.* **57**, 1013 (1986).

² M. Göppert-Mayer, *Ann. Phys. (Leipzig)* **9**, 273 (1931).

³ J. J. Hopfield, J. M. Worlock, and K. Park, *Phys. Rev. Lett.* **11**, 414 (1963).

⁴ H. Mahr, in *Quantum Electronics*, edited by H. Rabin and C. L. Tang (Academic Press, New York, 1975), Vol. 1A, pp. 285–361; D. Fröhlich (unpublished).

⁵ D. Fröhlich, E. Mohler, and P. Wiesner, *Phys. Rev. Lett.* **26**, 554 (1971).

⁶ Y. Masumoto, T. Kawamura, and K. Era, *Appl. Phys. Lett.* **62**, 225 (1993).

⁷ G. F. Koster, J. O. Dimmock, R. G. Wheeler, and H. Statz, *Properties of the Thirty-Two Point Groups* (MIT Press, Cambridge, MA, 1963).

⁸ K. Shindo, A. Morita, and H. Kamimura, *J. Phys. Soc. Jpn.* **20**, 2054 (1965); **20**, 2748(E) (1965).

⁹ A. Blacha, M. Cardona, N. E. Christensen, S. Ves, and H. Overhof, *Solid State Commun.* **43**, 183 (1982); *Physica B & C* **117B** & **118B**, 63 (1983).

¹⁰ M. Cardona, *Phys. Rev.* **129**, 69 (1963).

¹¹ A. Blacha, S. Ves, and M. Cardona, *Phys. Rev. B* **27**, 6346 (1983).

¹² A. L. Edwards and H. G. Drickamer, *Phys. Rev.* **122**, 1149 (1961).

¹³ H. Müller, S. Ves, H. D. Hochheimer, M. Cardona, and A. Jayaraman, *Phys. Rev. B* **22**, 1052 (1980).

¹⁴ S. Ves, D. Glötzel, M. Cardona, and H. Overhof, *Phys. Rev. B* **24**, 3073 (1981).

¹⁵ A. Blacha, N. E. Christensen, and M. Cardona, *Phys. Rev. B* **33**, 2413 (1986).

¹⁶ B. Staginnus, D. Fröhlich, and T. Caps, *Rev. Sci. Instrum.* **39**, 1129 (1968).

¹⁷ S. Suga and T. Koda, *Phys. Status Solidi B* **66**, 255 (1974).

¹⁸ G. Huber, K. Syassen, and W. B. Holzapfel, *Phys. Rev. B* **15**, 5123 (1977).

¹⁹ G. J. Piermarini, S. Block, J. D. Barnett, and R. A. Forman, *J. Appl. Phys.* **46**, 2774 (1975).

²⁰ H. K. Mao, P. M. Bell, J. W. Shaner, and D. J. Steinberg, *J. Appl. Phys.* **49**, 3276 (1978).

- ²¹ K. Reimann and K. Syassen, *Phys. Rev. B* **39**, 11 113 (1989).
- ²² D. Fröhlich, W. Nieswand, and St. Rübenacke, *J. Lumin.* (to be published).
- ²³ For excitons the binding energy depends on the dielectric constant and on the reduced mass of the exciton. Because of large valence-band masses the reduced mass is determined almost exclusively by the conduction-band mass. Since the conduction band is the same for $Z_{1,2}$ and Z_3 excitons, the assumption of equal binding energies is justified.
- ²⁴ K. K. Bajaj, *Phys. Status Solidi B* **64**, K107 (1974).
- ²⁵ A. Goldmann, *Phys. Status Solidi B* **81**, 9 (1977).
- ²⁶ G. L. Bir and G. E. Pikus, *Symmetry and Strain-Induced Effects in Semiconductors* (Wiley, New York, 1974).
- ²⁷ A. Blacha, H. Presting, and M. Cardona, *Phys. Status Solidi B* **126**, 11 (1984).
- ²⁸ R. C. Hanson, K. Helliwell, and C. Schwab, *Phys. Rev. B* **9**, 2649 (1974).
- ²⁹ T. H. K. Barron, J. A. Birch, and G. K. White, *J. Phys. C* **10**, 1617 (1977).
- ³⁰ F. H. Pollak, *Surf. Sci.* **37**, 863 (1973).
- ³¹ J. B. Anthony, A. D. Brothers, and D. W. Lynch, *Phys. Rev. B* **5**, 3189 (1972).
- ³² D. Fröhlich, W. Nieswand, and St. Rübenacke, *Phys. Rev. B* **47**, 6736 (1993).
- ³³ R. C. Hanson, J. R. Hallberg, and C. Schwab, *Appl. Phys. Lett.* **21**, 490 (1972).
- ³⁴ H. D. Hochheimer, M. L. Shand, J. E. Potts, R. C. Hanson, and C. T. Walker, *Phys. Rev. B* **14**, 4630 (1976).
- ³⁵ Y. Nozue and M. Ueta, *Solid State Commun.* **36**, 781 (1980).
- ³⁶ C. Wecker, A. Daunois, J. L. Deiss, P. Fiorini, and J. C. Merle, *Solid State Commun.* **31**, 649 (1979).